

Large spontaneous polarization in polar perovskite of $\text{PbTiO}_3\text{-Bi}(\text{Zn}_{1/2}\text{Ti}_{1/2})\text{O}_3$

Zhao Pan,^{a,b,c} Xingxing Jiang,^d Jun Chen,^{*,b} Lei Hu,^b Hajime Yamamoto,^c Linxing Zhang,^b Longlong Fan,^b Xi'an Fan,^a Yawei Li,^a Guangqiang Li,^a Yang Ren,^e Zheshuai Lin,^d Masaki Azuma^c and Xianran Xing^b

$\text{PbTiO}_3\text{-Bi}(\text{Zn}_{1/2}\text{Ti}_{1/2})\text{O}_3$ is considered to be a promising high-ferroelectric performance material in the Pb/Bi-based perovskite family. In the present study, a whole set of $(1-x)\text{PbTiO}_3\text{-}x\text{Bi}(\text{Zn}_{1/2}\text{Ti}_{1/2})\text{O}_3$ ($0 \leq x \leq 1$) solid solutions have been prepared by the conventional solid-state and high-pressure *vs* high-temperature methods. The effect of $\text{Bi}(\text{Zn}_{1/2}\text{Ti}_{1/2})\text{O}_3$ on the crystal structure has been investigated by synchrotron X-ray powder diffraction. Unlike most PbTiO_3 -based perovskites, the present system exhibits a continuously enhanced tetragonality (c/a) and large spontaneous polarization (P_s) properties. The enhanced c/a is ascribed to the large spontaneous polarization displacements induced by the strong Pb/Bi-O hybridization and coupling interactions between Ti/Zn and Pb/Bi cations, which can be evidenced by the lattice dynamics study and first-principles calculations. Accordingly, the T_c (i.e., $x = 0.5$) is expected to be approximately 1000 $^\circ\text{C}$ if its perovskite structure can be stabilized. The present study provides a route to obtain large- P_s in PbTiO_3 -based ferroelectric materials by introducing isostructural perovskites with strong polarity.

Introduction

It is well known that PbTiO_3 (PT) is a typical ABO_3 perovskite-type ferroelectric with a spontaneous polarization (P_s) parallel to the polar direction of the c axis.^{1,2} PT can easily form solid solutions with simple perovskites such as SrTiO_3 , BaTiO_3 , and PbZrO_3 , and complex lead-based compounds such as $\text{Pb}(\text{Mg}_{1/3}\text{Nb}_{2/3})\text{O}_3$ and $\text{Pb}(\text{Zn}_{1/3}\text{Nb}_{2/3})\text{O}_3$.³⁻⁵ However, the values of P_s are generally reduced with respect to PT ($P_s = 59 \mu\text{C}/\text{cm}^2$).⁶ Ferroelectric materials with large P_s are widely used in nonvolatile ferroelectric random access memories (FeRAM) and micro-electro-mechanical systems (MEMS) due to their high ferroelectric performance. Therefore, it is essential to improve the ferroelectricity of PT with large- P_s in order to meet the demand of ferroelectric applications.

It is proposed that the ferroelectric activity of A/B site cations play a crucial role in achieving high polarization in ferroelectrics.⁷ Several simple perovskites with ferroelectric-active cations such as BiFeO_3 (BF) and $\text{Bi}(\text{Zn}_{0.5}\text{Ti}_{0.5})\text{O}_3$ (BZT) are reported to exhibit strong polarity.^{8,9} Especially, polar perovskite of BZT, in which the B -site are occupied by the strong ferroelectric-active cations of Zn^{2+} and Ti^{4+} , has been reported to exhibit a P_s as large as $103 \mu\text{C}/\text{cm}^2$, which is much higher than that of BF ($60 \mu\text{C}/\text{cm}^2$) and PT.⁸ The large polarization leads to an extremely high lattice distortion (c/a) of 1.21 of BZT.⁹ Nevertheless, BZT exhibits poor chemical stability and tends to decompose at temperatures far below its Curie temperature (T_c).¹⁰ Inspired by the remarkable ferroelectric properties in the solid solutions between PT and simple perovskite of BiScO_3 ,¹¹ a high ferroelectric performance could also be expected in the binary solid solutions of PT-BZT. Previous studies have suggested a continuously enhanced tetragonality of $(1-x)\text{PT-}x\text{BZT}$ up to $x = 0.40$, indicating the potential large ferroelectric polarization in present system.¹² However, the solid solubility of BZT in PT is limited to 40 mol% at ambient condition, and it is difficult to obtain the whole solid solutions by traditional solid-state method. A larger ferroelectric polarization can be foreseeable if its solid solubility can be improved.

^a State key laboratory of refractories and metallurgy, Wuhan University of Science and Technology, Wuhan 430081, China.

^b Department of Physical Chemistry, University of Science and Technology Beijing, Beijing 100083, China. E-mail: junchen@ustb.edu.cn; Fax: +86 10 62332525; Tel: +86 10 82375027.

^c Materials and Structures Laboratory, Tokyo Institute of Technology, 4259 Nagatsuta, Midori, Yokohama, 226-8503, Japan

^d Center for Crystal R&D, Key Laboratory of Functional Crystals and Laser Technology, Technical Institute of Physics and Chemistry, Chinese Academy of Sciences, Beijing 100190, China

^e X-Ray Science Division, Argonne National Laboratory, Argonne, Illinois 60439, United States.

[†] Footnotes relating to the title and/or authors should appear here.

Electronic Supplementary Information (ESI) available: Rietveld refinement of the synchrotron X-ray diffraction patterns of $(1-x)\text{PbTiO}_3\text{-}x\text{Bi}(\text{Zn}_{1/2}\text{Ti}_{1/2})\text{O}_3$ ($x = 0.1, 0.2, 0.3, 0.4, 0.5$, and 0.6), See DOI: 10.1039/x0xx00000x

Herein, the present work aims at increasing the solid solubility between BZT and PT by high-pressure *vs* high-temperature (HPHT) method, in order to further investigate the ferroelectric polarization property of $(1-x)\text{PT-}x\text{BZT}$ system. The crystal structure, lattice dynamics, and related ferroelectric properties have been studied systematically by the joint experimental and theoretical investigations.

Experiment

Materials and synthesis

(1-x)PT-xBZT ($x = 0.1 - 1.0$) solid solutions were synthesized by using the conventional solid-state ($x \leq 0.4$) and HPHT ($x > 0.4$) methods. The details of sample preparation utilizing the traditional solid-state method were provided in previous studies.¹³ Due to the metastable nature of BZT, compounds for $x > 0.4$ were fabricated by HPHT method. Samples in the solutions series of (1-x)PT-xBZT ($x > 0.4$) were prepared from a stoichiometric mixture of PbO, TiO₂, Bi₂O₃, and ZnO. The mixture was carefully ground in a glove box and sealed in a gold capsule, then treated at 6 GPa and 1100 °C for 30 min in a cubic-anvil type high-pressure apparatus. After the high pressure synthesis, the samples were carefully ground and annealed at 400 °C for 1 h and slowly cooled to room temperature in order to remove the mechanical strain introduced during the high pressure process.

Measurements

The X-ray diffraction (XRD) patterns were collected with the Bruker D8 ADVANCE diffractometer for phase identification. In order to precisely determine the detailed crystal structure, the high energy synchrotron X-ray diffraction (SXRD) facility was used at the 11-ID-C beamline of the Advanced Photon Source with the light wavelength of 0.11725 Å and the BL44B2 beamline of SPring-8 with the light wavelength of 0.5 Å. The SXRD data were refined using the Rietveld method supported by the FullProf software with the same initial model as for PT (*P4mm*, No. 99). Raman scattering spectra were collected on a JY-T64000 Raman spectrometer (Jobin Yvon, France) at room temperature.

Computational method

The first-principles calculations were performed by CASTEP,¹⁴ a total energy program based plane-wave pseudopotential density functional theory (DFT).¹⁵ The generalized gradient approximation (GGA)¹⁶ functionals of Perdew-Burke-Ernzerhof (PBE)¹⁷ was employed to describe the exchange-correlation energy. The effective interaction between the atomic cores and valence electrons were modelled by optimized normconserving pseudopotential¹⁸ in Kleinman-Bylander form.¹⁹ Virtual crystal approximation (VCA)²⁰ was adopted to deal with the Zn/Ti and Pb/Bi disorder in 0.5PbTiO₃-0.5BiZn_{1/2}Ti_{1/2}O₃, in which the pseudo-atoms were created with the Coulomb potential in proportion to the element composition in the disordered sites. Kinetic energy cutoff of 900 eV and Monkhorst-Pack²¹ *k*-point mesh spanning less than 0.03 Å⁻¹ in the Brillouin zone were chosen. Tests showed that the above computational parameters and methodology are sufficiently accurate for the current study.

Results and Discussion

The structure evolution of (1-x)PT-xBZT ($x = 0.1-1$) solid solutions are shown in Fig. 1(a). The samples are in high purity without any detectable impurities. It can be seen that the full-range solid solutions of (1-x)PT-xBZT with perovskite structure are obtained. All the investigated samples are indexed into the same tetragonal symmetry as that of PT. With increasing content of BZT, the (001) peaks gradually shift to the lower angles while the (100) ones shift to the higher ones. This indicates the expansion of the *c* axis and the

shrinkage of the *a* axis. The detailed evolutions of lattice parameters are depicted in Fig. 1(b). With the introduction of BZT, it can be observed that the *c* axis of (1-x)PT-xBZT increases almost linearly, whereas the *a*(*b*) axis shows an opposite trend, leading to an unusually enhanced tetragonality (*c/a*). Note that most chemical substituted PT-based solid solutions typically exhibit a weakened *c/a*,

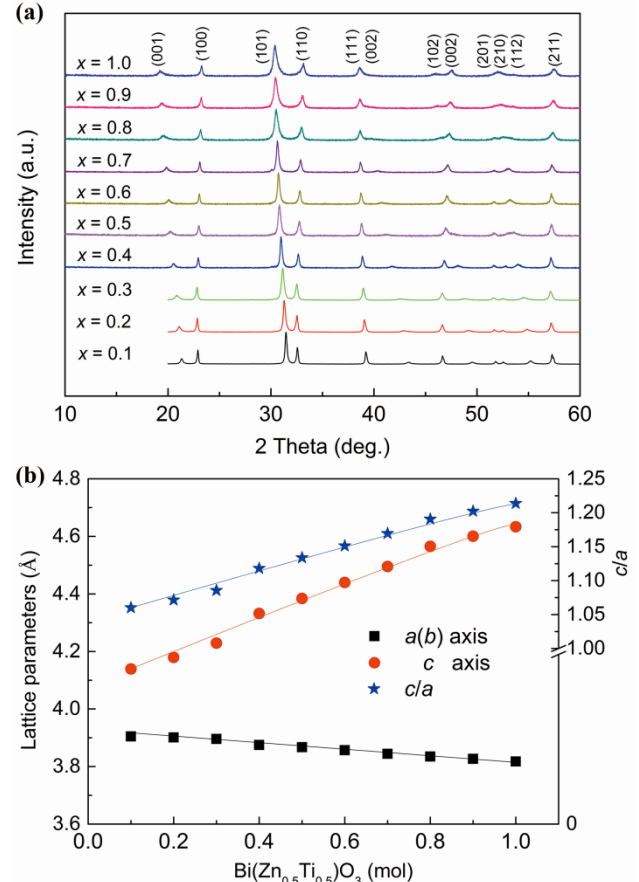


Figure 1 (a) XRD patterns and (b) lattice parameters of (1-x)PT-xBZT ($x = 0.1 - 1.0$) at room temperature.

such as with BaTiO₃, SrTiO₃, Pb(Mg_{1/3}Nb_{2/3})O₃, and Pb(Zn_{1/3}Nb_{2/3})O₃, and most Pb/Bi-based systems of PT-Bi(Ni_{1/2}Ti_{1/2})O₃, PT-Bi(Ni_{2/3}Nb_{1/3})O₃, PT-Bi(Mg_{1/2}Ti_{1/2})O₃.³⁻⁵ Only few of them show abnormally enhanced tetragonality (*c/a*), such as the present PT-BZT, PT-BF, and recently reported PT-Bi(Zn_{1/2}Hf_{1/2})O₃ and PT-PbVO₃.^{12,22-24} Here, the *c/a* increases from 1.06 for pure PT, to as large as 1.13 for 0.5PT-0.5BZT, and finally reaches up to 1.21 for pure BZT. The enhanced tetragonality should be closely related to the large *P_s* displacements induced by the strong Pb/Bi-O hybridization and coupling interactions between Ti/Zn and Pb/Bi cations.^{25,26} Generally, large tetragonality in the PT-based piezoelectric materials is usually accompanied by intriguing physical scenarios such as large *P_s* and high *T_C*.

It is interesting to observe that the large tetragonality is accompanied with a pyramidal rather than an octahedral coordination of Ti/Zn-O in the (1-x)PT-xBZT solid solutions (Fig. 2(a)). In order to obtain information about *P_s*, the detailed structural information was extracted by the Rietveld method (Supporting

Information, Fig. S1-S10). In ABO_3 perovskite-type ferroelectric, the P_s originates from the displacements of the A site Pb/Bi or B site Ti/Zn atoms away from the centroid of the oxygen polyhedra, respectively (Fig. 2(b)). The value of P_s can be estimated by considering a pure

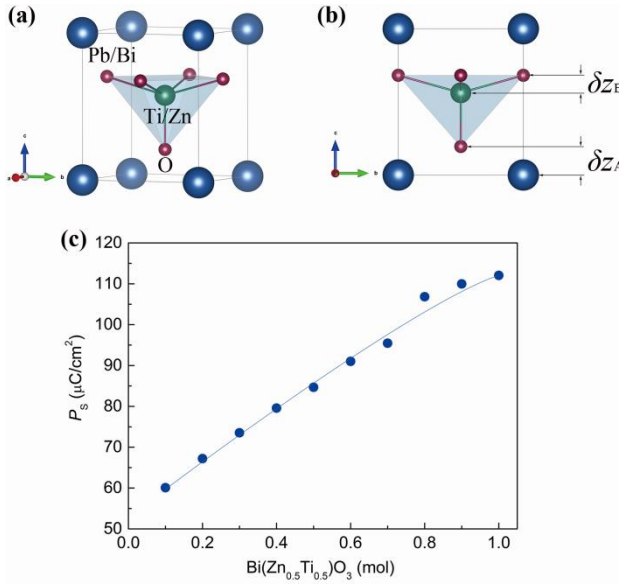


Figure 2 (a) The crystal structure, (b) the schematic diagram of P_s displacement, and (c) the calculated spontaneous polarization of $(1-x)PT-xBZT$ ($x = 0.1 - 1.0$).

ionic crystal and neglecting the electronic polarization contribution.²⁷ Here the P_s displacements of A site (δz_A) and B site (δz_B) can be derived from SXRD. As it can be seen, both δz_A and δz_B show a nearly linear increase as a function of the BZT content (Fig. S11). Correspondingly, P_s is gradually enhanced by the chemical substitution of BZT, ranging from $59 \mu\text{C}/\text{cm}^2$ for pure PT, to $85 \mu\text{C}/\text{cm}^2$ for $0.5PT-0.5BZT$, and finally to as large as $112 \mu\text{C}/\text{cm}^2$ for pure BZT (Fig. 2(c)). The present compounds of $(1-x)PT-xBZT$ exhibit giant ferroelectric polarization property, which is much higher than those of most representative ferroelectrics, such as simple perovskites of PT ($59 \mu\text{C}/\text{cm}^2$) and $BiFeO_3$ ($60 \mu\text{C}/\text{cm}^2$).^{6,8} It is even comparable with the strong polar perovskites of $BiCoO_3$ ($120 \mu\text{C}/\text{cm}^2$) and $PbVO_3$ ($101 \mu\text{C}/\text{cm}^2$).^{28,29} According to the Landau theory, defined as $T_C = \alpha P_s^2$,⁶ the present $(1-x)PT-xBZT$ should be a promising high- T_C piezoelectric material. If taking PT as a reference for the calculation ($P_s = 59 \mu\text{C}/\text{cm}^2$, $T_C = 490^\circ\text{C}$), the T_C of $0.5PT-0.5BZT$ could be approximately 1000°C .

According to the lattice dynamical theory, the vibrational soft modes are suggested to be associated with the ferroelectric phase transition. The study of lattice dynamics suggests that the frequency of $A_1(1TO)$ soft mode is proportional to the order parameter P_s due to it represents the displacement of the TiO_6 octahedron relative to Pb atoms.³⁰ The $A_1(1TO)$ soft mode is almost linear with the displacement of A-site atoms, which can indicate the variation of P_s in PT-based compounds both with normally reduced c/a and abnormally enhanced c/a .^{31,32} For example, an enhanced c/a together with hardened $A_1(1TO)$ have been observed in $Pb_{1-x}Cd_xTiO_3$, while an opposite tendency of a reduced c/a and softened $A_1(1TO)$ have been observed in $Pb_{1-x}Sr_xTiO_3$.^{33,34} Apart from the $A_1(1TO)$, the

$A_1(2TO)$ soft mode is sensitive to the P_s displacement of B-site atoms since it consists of the displacement of B-site atoms relative to the oxygen and A-site atoms.³⁵ The Raman spectra and the soft modes of the present $(1-x)PT-xBZT$ solid solutions are shown in Fig. 3(a). Interestingly, the Raman active modes of $A_1(1TO)$ and $A_1(2TO)$ abnormally shift to higher frequency with increasing BZT content (Fig. 3(b)), indicating the enhanced P_s displacements in both A-site and B-site. These are consistent with the structure refinements from SXRD

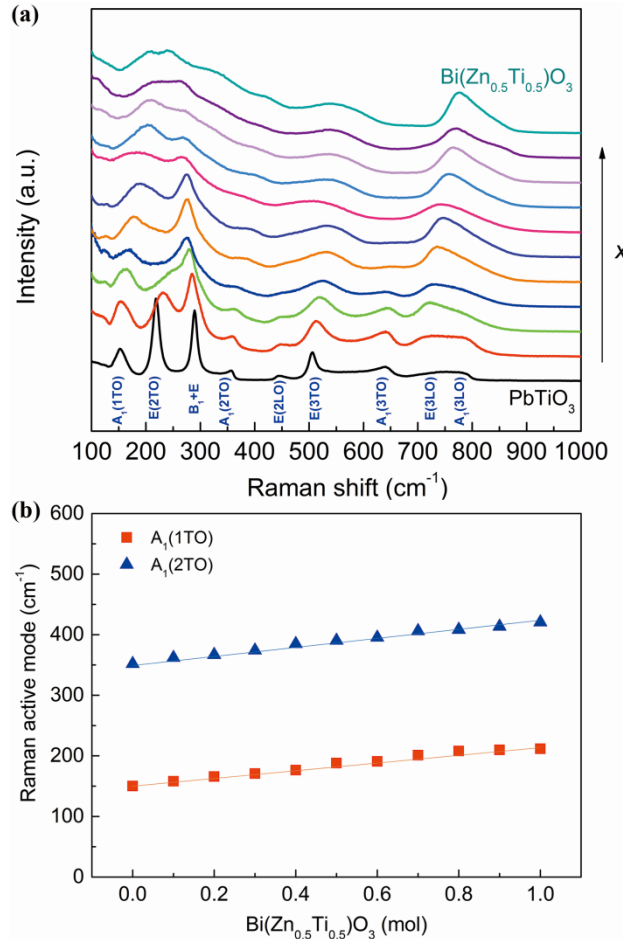


Figure 3 (a) Raman spectra and (b) Raman active modes of $(1-x)PT-xBZT$ ($x = 0.0 - 1.0$) solid solutions as a function of x .

as mentioned before. Note that these optical modes of $A_1(1TO)$ and $A_1(2TO)$ are generally softened in any other PT-based systems with a reduced c/a , such as in $Pb_{1-x}Sr_xTiO_3$, $PbZr_{1-x}Ti_xO_3$, and $(1-x)PT-xPb(Mg_{1/3}Nb_{2/3})O_3$.^{34,36,37} Since the A-site Pb/Bi atoms and BO_6 octahedron vibrates in the opposite direction, a simple harmonic model of $\omega = \sqrt{k/m^*}$ can be applied to study the effect of the substitution of BZT for PT on the frequency ω of Raman active mode. Correspondingly, k is the force constant related to the Pb/Bi-O bond strengths and m^* is the reduced mass of Raman active mode. In the whole set of $(1-x)PT-xBZT$ solid solutions, the m^* is close due to the similar mass of Pb and Bi atoms. Hence, the upward shift of $A_1(1TO)$ and $A_1(2TO)$ optical modes is mainly attributed to the enhanced force constant k of Pb/Bi-O bonds derived from the strong hybridization between Pb/Bi and O atoms. In addition, the large P_s displacement of A-site cations is also favored by the coupling with that of B-site

cations. The *B*-sites of $(1-x)$ PT- x BZT are occupied by the strong ferroelectric active cations of Ti and Zn, which can form short and strong covalent bonds between Ti/Zn with O.³⁸ These strong covalent bonds between cations and oxygen enhance the force constant k of Raman modes and thus harden these modes of $A_1(1\text{TO})$ and $A_1(2\text{TO})$.

To further study the effect of Bi/Pb and Zn/Ti substitution on hybridization with oxygen atoms, the electron density difference of PT and 0.5PT-0.5BZT was calculated by first-principles calculations (Fig. 4). Accordingly, it is observed that in undoped PT, the considerable loss of the electronic cloud density in the near-bond area occurs during the chemical bond formation (Fig. 4(a)). In comparison, in 0.5PT-0.5BZT, the electronic cloud is transferred from the near-oxygen to near-Zn/Ti area, and a large amount of electronic cloud is concentrated around bond (Fig. 4(b)). This stark distinction strongly manifests the enhancement of Bi/Pb and Zn/Ti substitution on the orbital hybridization, which is in good agreement with the conclusion deduced from the experimentally observed result.

The present work provides a way for exploring high ferroelectric performance materials by introducing the strong polar perovskites in PT-based ferroelectrics. Based on these, we propose that other unreported PT-based solid solutions containing polar perovskites, such as BiCoO₃ and Bi(Zn_{1/2}V_{1/2})O₃,^{28,29} should also exhibit enhanced tetragonality and large ferroelectric polarization. Furthermore, since the present $(1-x)$ PT- x BZT solid solutions exhibit large P_s , promising ferroelectric properties could be expected if the perovskite structure can be stabilized, such as by growing epitaxial thin films. It needs to be mentioned that PT-based perovskites with large lattice distortion could also induce other intriguing physical properties such as colossal volume contraction as reported in Pb(Ti, V)O₃.²⁴

Conclusions

In summary, a comprehensive study of $(1-x)$ PT- x BZT solid solutions has been conducted. A whole set of $(1-x)$ PT- x BZT ($0 \leq x \leq 1$) solid solutions have been synthesized by the conventional solid-state and high-pressure vs high-temperature methods. The system exhibits a continuous enhanced tetragonality and large P_s from $x = 0$ for PT up to $x = 1.0$. The enhanced tetragonality is attributed to the large P_s displacements induced by the strong Pb/Bi-O hybridization and coupling interactions

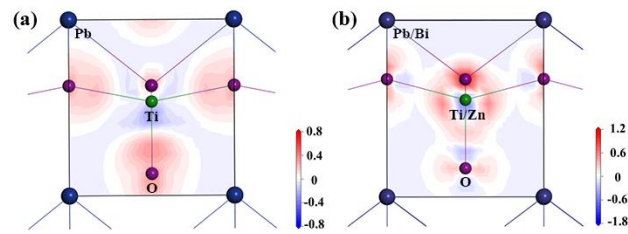


Figure 4 The electron density difference map of (a) PT and (b) 0.5PT-0.5BZT. The Pb(Pb/Bi), Ti(Zn/Ti) and O atoms are represented by black-blue, green and violet balls, respectively.

between Ti/Zn and Pb/Bi cations, as evidenced by the Raman study and first-principles calculations. The giant calculated P_s in $(1-x)$ PT- x BZT suggests its potential as high ferroelectric performance and high- T_c piezoelectric materials. The present study provides an approach to exploring and designing high- T_c piezoelectric materials by intentionally introducing strong polar perovskites into PT.

Acknowledgements

This work was supported by the National Natural Science Foundation of China (Grant Nos. 21731001 and 21590793), National Program for Support of Top-notch Young Professionals, the Program for Chang Jiang Young Scholars, the Fundamental Research Funds for the Central Universities, China (FRF-TP-17-001B), and the General Financial Grant from the China Postdoctoral Science Foundation (2017M622536). This research used resources of the Advanced Photon Source, a U.S. Department of Energy (DOE) Office of Science User Facility operated for the DOE Office of Science by Argonne National Laboratory under Contract No. DE-AC02-06CH11357. The room temperature synchrotron radiation experiments also performed at the BL44B2 beamline of SPring-8 with the approval of the Japan Synchrotron Radiation Research Institute (JASRI) (Proposal NO. 2016A1060).

Notes and references

- 1 B. Jaffe, W. R. Cook and H. Jaffe, *Piezoelectric Ceramics*. Academic, London-New York, 1971.
- 2 J. Chen, L. Hu, J. X. Deng and X. R. Xing, *Chem. Soc. Rev.*, 2015, **44**, 3522.
- 3 X. R. Xing, J. Chen, J. X. Deng and G. R. Liu, *J. Alloy. Compd.*, 2003, **360**, 286.
- 4 X. R. Xing, J. X. Deng, Z. Q. Zhu and G. R. Liu, *J. Alloy. Compd.*, 2003, **353**, 1.
- 5 G. H. Haerting, *J. Am. Ceram. Soc.*, 1999, **82**, 797.
- 6 S. C. Abrahams, S. K. Kurtz and P. B. Jamieson, *Phys. Rev.*, 1968, **172**, 551.
- 7 I. Grinberg, A. M. Rappe, *Phase Transitions*, 2007, **80**, 351.
- 8 G. Catalan and J. F. Scott, *Adv. Mater.*, 2009, **21**, 2463.
- 9 M. R. Suchomel, A. M. Fogg, M. Allix, H. Niu, J. B. Claridge and M. J. Rosseinsky, *Chem. Mater.*, 2006, **18**, 4987.
- 10 Z. Pan, J. Chen, R. Yu, H. Yamamoto, Y. Rong, L. Hu, Q. Li, K. Lin, L. You, K. Zhao, L. Fan, Y. Ren, K. Kako, M. Azuma, X. Xing, *Inorg. Chem.*, 2016, **55**, 9513.
- 11 R. E. Eitel, C. A. Randall, T. R. Shrout and S. -E. Park, *Jpn. J. Appl. Phys.*, 2002, **41**, 2099.
- 12 M. R. Suchomel and P. K. Davies, *Appl. Phys. Lett.*, 2005, **86**, 262905.
- 13 Z. Pan, J. Chen, L. L. Fan, L. J. Liu, L. Fang and X. R. Xing, *J. Appl. Phys.*, 2012, **112**, 114120.
- 14 S. J. Clark, M. D. Segall, C. J. Pickard, P. J. Hasnip, M. J. Probert, K. Refson and M. C. Payne, *Z. Kristallogr.*, 2005, **220**, 567.
- 15 M. C. Payne, M. P. Teter, D. C. Allan, T. A. Arias and J. D.

Joannopoulos, *Rev. Mod. Phys.*, 1992, **64**, 1045.

¹⁶ J. P. Perdew and Y. Wang, *Phys. Rev. B*, 1992, **46**, 12947.

¹⁷ J. P. Perdew, K. Burke and M. Ernzerhof, *Phys. Rev. Lett.*, 1996, **77**, 3865.

¹⁸ D. R. Hamann, M. Schluter and C. Chiang, *Phys. Rev. Lett.*, 1979, **43**, 1494.

¹⁹ L. Kleinman and D. M. Bylander, *Phys. Rev. Lett.*, 1982, **48**, 1425.

²⁰ L. Bellaiche and D. Vanderbilt, *Phys. Rev. B*, 2000, **61**, 7877.

²¹ H. J. Monkhorst and J. D. Pack, *Phys. Rev. B*, 1976, **13**, 5188.

²² D. I. Woodward, I. M. Reaney, R. E. Eitel and C. A. Randall, *J. Appl. Phys.*, 2003, **94**, 3313.

²³ Z. Pan, J. Chen, L. L. Fan, H. Liu, L. X. Zhang, L. Hu, Y. Ren, L. J. Liu, L. Fang, X. A. Fan, Y. W. Li and X. R. Xing, *Inorg. Chem. Front.*, 2017, **4**, 1352.

²⁴ Z. Pan, J. Chen, X. X. Jiang, L. Hu, R. Z. Yu, H. Yamamoto, T. Ogata, Y. Hattori, F. M. Guo, X. A. Fan, Y. W. Li, G. Q. Li, H. Z. Gu, Y. Ren, Z. S. Lin, M. Azuma and X. R. Xing, *J. Am. Chem. Soc.*, 2017, **139**, 14865.

²⁵ J. Chen, X. Y. Sun, J. X. Deng, Y. Zou, Y. T. Liu, J. H. Li and X. R. Xing, *J. Appl. Phys.*, 2009, **105**, 044105.

²⁶ Z. Pan, J. Chen, X. X. Jiang, Z. S. Lin, L. X. Zhang, L. L. Fan, Y. C. Rong, L. Hu, H. Liu, Y. Ren, X. J. Kuang and X. R. Xing, *Inorg. Chem.*, 2017, **56**, 2589.

²⁷ H. Liu, J. Chen, X. X. Jiang, Z. Pan, L. X. Zhang, Y. C. Rong, Z. S. Lin and X. R. Xing, *J. Mater. Chem. C*, 2017, **5**, 931.

²⁸ K. Oka, M. Azuma, W. T. Chen, H. Yusa, A. A. Belik, E. Takayama-Muromachi, M. Mizumaki, N. Ishimatsu, N. Hiraoka, M. Tsujimoto, M. G. Tucker, J. P. Attfield and Y. Shimakawa, *J. Am. Chem. Soc.*, 2010, **132**, 9438.

²⁹ R. Z. Yu, H. Hojo, K. Oka, T. Watanuki, A. Machida, K. Shimizu, K. Nakano and M. Azuma, *Chem. Mater.*, 2015, **27**, 2012.

³⁰ G. Burns and B. A. Scott, *Phys. Rev. Lett.*, 1970, **25**, 167.

³¹ G. Burns and B. A. Scott, *Phys. Rev. B*, 1973, **7**, 3088.

³² J. Chen, P. H. Hu, X. Y. Sun, C. Sun and X. R. Xing, *Appl. Phys. Lett.*, 2007, **91**, 171907.

³³ J. Chen, X. R. Xing, R. B. Yu, G. R. Liu, J. H. Li and Y. T. Liu, *J. Appl. Phys.*, 2006, **100**, 074106.

³⁴ S. Y. Kuo, C. T. Li and W. F. Hsieh, *Appl. Phys. Lett.*, 2002, **81**, 3019.

³⁵ M. K. Singh, S. Ryu and H. M. Jang, *Phys. Rev. B*, 2005, **72**, 132101.

³⁶ G. Burns and B. A. Scott, *Phys. Rev. Lett.*, 1970, **25**, 1191.

³⁷ H. Ohwa, M. Iwata, H. Orihara, N. Yasuda and Y. J. Ishibashi, *J. Phys. Soc. Jpn.*, 2001, **70**, 3149.

³⁸ I. Grinberg, M. R. Suchomel, W. Dmowski, S. E. Mason, H. Wu, P. K. Davies and A. M. Rappe, *Phys. Rev. Lett.*, 2007, **98**, 107601.